

Interfacial stability and atomistic processes in the *a*-C/Si(100) heterostructure system

P. C. Kelires

*Physics Department, University of Crete, P.O. Box 2208, 710 03 Heraklion, Crete, Greece
and Foundation for Research and Technology-Hellas (FORTH), P.O. Box 1527, 711 10, Heraklion, Crete, Greece*

M. Gioti and S. Logothetidis

*Physics Department, Aristotle University of Thessaloniki, GR-54006 Thessaloniki, Greece
(Received 26 May 1998)*

We study the interfacial properties of thin amorphous carbon films grown on silicon (100) substrates. By combining experimental spectroscopic ellipsometry and stress measurements and theoretical Monte Carlo simulations, we show that significant interdiffusion takes place at the initial stages of growth, driven by a strain mediated mechanism, and we identify the relevant atomistic processes. [S0163-1829(99)06507-8]

I. INTRODUCTION

The quantitative description of amorphous thin films, which are usually grown on top of crystalline substrates, manifests a high level of complication introduced by the presence of the *amorphous/crystalline* interface. Because realization of such thin films is vigorously pursued for a wide range of technological applications, it is very important to understand the interfacial properties of these systems. It seems to be essential for the designing and development of good-quality films. Until now, however, most studies have been restricted to exploring the properties of deposited films as a function of substrate conditions, neglecting the interface factor.

The growth of highly tetrahedral amorphous carbon (ta-C) films offers a good example in this respect. It is well known that the substrate temperature and bias strongly influence the structural and electronic properties of such films. However, little is known about the *microscopic* aspects of the problem, especially at the initial stages of growth. Thus, the interaction of the growing amorphous film with the underlying crystalline substrate, and the atomistic processes taking place at their interface, are not adequately investigated. We believe that this interaction is important for the development of thicker films with the desired properties, and insight into this issue is therefore essential to obtain.

Here, we address the stability problem and the fundamental question of whether or not there is interdiffusion of species at the interface of thin-layer *a*-C films with Si(100), one of the most commonly used substrates. Such investigations have been previously carried out only for crystalline semiconductor heterostructures and superlattices.¹ Our studies were instigated after the characterization of several *a*-C ultrathin films grown with the rf magnetron sputtering technique.² Using spectroscopic ellipsometry (SE) and stress measurements as the experimental probe, as well as theoretical Monte Carlo (MC) simulations, we have been able to show that indeed intermixing is taking place. We find that C atoms diffuse into the substrate, occupying substitutional positions and forming SiC-like local geometries, while Si atoms enter into the thin amorphous layer. We explain and investigate the consequences of these findings.

In the following sections, we outline first our experimental and theoretical methods of investigation. We then give our experimental results regarding the dielectric and stress properties of the film/substrate composite structures, which indicate intermixing of species across the interface. Next, we describe theoretical simulations that confirm the experimental conclusions, and we discuss possible factors that lead to interdiffusion. Finally, we give our conclusions.

II. METHODOLOGY

A. Experimental details

The *a*-C films were deposited on Si(100) wafers from a graphite target with the rf magnetron sputtering technique using the Alcatel SCM600 deposition system. The base pressure of the main deposition chamber was as low as 1×10^{-7} mbar. A phase-modulated ellipsometer attached on the deposition system at an angle of incidence of 70.4° was used for real-time and *in situ* SE measurements in the energy region of 1.5–5.5 eV. The Si substrates were cleaned in air with a standard surface cleaning procedure, whereas a low-energy dry ion (Ar^+) etching process was used in vacuum to remove the native SiO_2 . The process was monitored with real-time ellipsometry. The discharge power at the graphite (99.999% purity) target was kept constant at 100 W, the Ar partial pressure at 2×10^{-2} mbar, and the substrate to target distance at 65 mm. During deposition, the applied bias voltage (V_b) onto the substrate was -20 V. All films were deposited at room temperature (RT).

For the purpose of our investigations two series of measurements were taken, both involving the sequential deposition of very thin *a*-C layers. In the first, *in situ* SE spectra were obtained after each layer was deposited. This was followed by exposure of the grown layer to atmospheric air, in order to perform stress measurements, after which SE spectra were taken again. The internal stress in the carbon films was derived from the curvature of the Si wafer, calculated through the modified Stoney's equation using a laser-based (Tencor Model 2320) instrument. The time interval between deposition of two successive layers was about 20 min, which amounts to the time to obtain the spectra, to unload (load) the sample from (into) the main chamber, and to mea-

sure the film stress. In the second series of experiments, *in situ* SE measurements were performed after each layer's deposition, without any exposure to air. Because of the Ar⁺ bombardment, the temperature of the structure is raised during deposition. For this reason, a time interval of at least 15 min was allowed between successive layers to keep the temperature close to RT.

Ellipsometry is a surface-sensitive, nondestructive technique that yields the complex reflection ratio $\rho = \tan \psi e^{i\Delta}$, through which the complex dielectric function $\epsilon(\omega) (= \epsilon_1 + i\epsilon_2)$ of a material is calculated.³ Analysis of the dielectric function enables one to obtain the film composition as well as to probe structural changes in the composite structure and focus on its individual parts. Photons with energies near ~ 4.3 eV (the E_2 structure of *c*-Si) have a small penetration depth (~ 80 Å) and are thus suitable to reveal changes in the thin *a*-C layer and near the interface area. On the other hand, photons with energies near ~ 3.3 eV (the E_1 structure of *c*-Si) have a larger penetration depth (~ 300 Å) and probe changes deeper in the substrate.

B. Theoretical methods

The theoretical atomistic simulations of the interface equilibrium structure are performed using a recently introduced by one of us state-of-the art Monte Carlo (MC) algorithm⁴ that includes, in addition to the usual random atomic displacements and volume changes, identity switches (from Si to C and *vice versa* in the present case) accompanied by appropriate relaxations of nearest-neighbor (nn) atoms. This effectively lowers the high barriers for diffusion in systems characterized by huge size mismatch between the constituent atoms. The statistical ensemble underlying this algorithm is the semigrand canonical (SGC) ensemble, which allows fluctuations in the number of atoms of each species (but keeping the total number of atoms N fixed) as a result of exchanges of particles within the system, driven by the appropriate chemical potential difference ($\Delta\mu = \mu_{\text{Si}} - \mu_{\text{C}}$, for the problem at hand).

The implementation of this ensemble for MC simulations, modified to include nn relaxations, is done through the Metropolis algorithm in the following way: The change in the potential energy of the heterostructure system at a given MC step is a sum of three terms,

$$\Delta U(s^N) = \Delta U_{\text{displ}}(s^N \rightarrow s'^N) + \Delta U_{\text{flip}}(s^N) + \Delta U_{\text{relax}}(s^N \rightarrow s'^N), \quad (1)$$

where s^N is symbolic for the $3N$ scaled atomic coordinates in the cell. The first term is the change due to random displacements, the second is due to identity flips, and the third is due to the accompanying relaxations. The traditional random atomic moves ($s^N \rightarrow s'^N$), and the volume changes $V \rightarrow V'$ are accepted with a probability

$$P_{\text{acc}} = \text{Min}[1, \exp(-\beta\Delta W)] \sim e^{-\Delta W/k_B T}, \quad (2)$$

where

$$\Delta W = \Delta U_{\text{displ}}(s^N \rightarrow s'^N) + P(V' - V) - Nk_B T \ln(V'/V), \quad (3)$$

as in the more familiar isobaric-isothermal (N, P, T) ensemble. For the trial moves that select one of the N particles at random, and with equal probability change its identity into one of the other possible identities of the system, the acceptance probability is given by

$$P_{\text{acc}}^{\text{iden}}(i \rightarrow i') = \text{Min} \left[1, \frac{\lambda_{i'}}{\lambda_i} \exp[-\beta\Delta U(s^N)] \right] \sim e^{\beta\Delta\mu} e^{-\beta\Delta U(s^N)}, \quad (4)$$

where $\lambda_i = e^{\mu_i/k_B T}$ are the fugacities in the system. $\Delta U(s^N)$ denotes the change in potential energy due to the identity ($i \rightarrow i'$) flip and the accompanying relaxations, so it is the combined effect of the last two terms in Eq. (1). This can be expressed more rigorously as

$$\Delta U(s^N) = E_{\text{cluster}} \left(i \rightarrow i', \sum_{k=1}^{nn} \sum_{j=1}^3 \Delta s_k^j(r_{0k}^j) \right) - E_{\text{cluster}}^0. \quad (5)$$

The energy is estimated over the cluster of atoms affected by the move and the relaxations before and after the move. Each nearest neighbor is relaxed away or towards the central atom (which changes identity from i to i' and is labeled 0) in the bond direction \vec{r}_{0k} . Further details on how the relaxations are performed can be found in a recent review article.⁵

For the present application it is desirable to work with a fixed composition in the composite structure. This is achieved by starting the simulation with the (N, P, T) ensemble and including identity flips in the form of *mutual particle interchanges* (from Si to C at a randomly chosen site and *vice versa* at another site). This is equivalent with removing the chemical potential term in Eq. (4). The interatomic interactions are modeled via the empirical potentials of Tersoff for multicomponent systems,⁶ which have been extensively tested and applied with success in similar contexts, both in strained semiconductor alloys^{4,7} as well as in simulations of *a*-C systems.⁸

For the simulations we use $(4 \times 3)(100)$ supercells consisting of a 24-layer *c*-Si substrate, on top of which a thin *a*-C layer is formed. The composite structures are periodically repeated in the two lateral dimensions that are constrained to be those of the Si lattice. To generate the thin amorphous films, an appropriate number of strained diamond layers are liquified at ~ 9000 K, and subsequently cooled to 300 K under pressure using the (N, P, T) ensemble. Pressures up to 200 GPa and cooling rates up to ~ 25 (MC steps)/atom K are used. After quenching the pressure is removed, the density of the composite structure is equilibrated, and the atomic positions are relaxed. During this first stage of simulations, the temperature of the substrate is kept constant at 300 K and intermixing of species across the interface is not allowed. In the second stage, we allow atom-identity flips to model possible interdiffusion. We equilibrate the composite structures by allowing diffusion of atoms within the whole *a*-C layer and within 18 substrate layers. Successful flips become considerable at ~ 600 K and above, which is consistent with actual deposition conditions in magnetron sput-

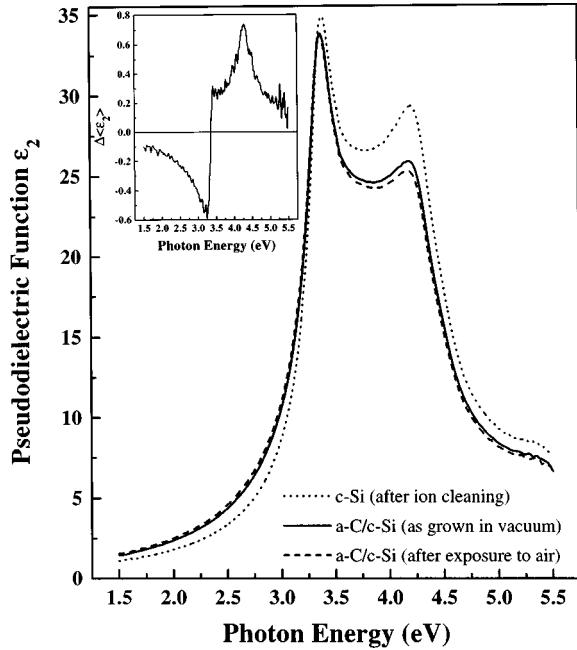


FIG. 1. Imaginary part of $\langle\epsilon\rangle$ of a typical composite structure (an 8-Å *a*-C film on *c*-Si). Solid line denotes the spectrum obtained in vacuum, while dashed line shows the spectrum obtained after exposure to air. Inset shows the differences between the two spectra. Also shown for comparison is the ϵ_2 of the *c*-Si substrate (dotted line) before deposition of the *a*-C film.

tering experiments, where the intense argon bombardment may raise locally the temperature in the thin film-interface region well beyond 1000 K.

III. RESULTS AND DISCUSSION

A. Experimental dielectric function and internal stresses

We first present our experimental findings. Figure 1 displays the imaginary part of the dielectric function (dotted line) of the *c*-Si(100) substrate after the ion cleaning procedure, and before the film deposition, and the pseudodielectric function ($\langle\epsilon\rangle$) of an ultrathin *a*-C layer grown on Si, obtained before (solid line) and after (dashed line) exposure to air. The contribution of the *a*-C film to this spectrum is clearly shown. It is also evident that the spectra obtained after the exposure to air exhibit a degradation when compared with those obtained from the as deposited film. The differences (shown in the inset) are mainly in the absolute $\langle\epsilon_2\rangle$ values, while the energy shift is below 1 meV. Since no other structural changes would lead to such degradation, the phenomenon is attributed to bulk oxidation of the *a*-C film and/or to the formation of SiO₂ surface units (overlayer). This can only be explained if Si atoms from the substrate force their way into the bulk, and even the surface, of the thin amorphous carbon layer during growth. Oxygen can then penetrate after air exposure into the film and form SiO₂-like geometries, replacing weaker Si-C bonds. We attribute the negative $\Delta\langle\epsilon_2\rangle$ values below ~ 3.2 eV to the SiO₂ overlayer, and to the fact that both *c*-Si and SiO₂ are transparent, which provides an apparent increase in $\langle\epsilon_2\rangle$ values. This increase is purely a phase or geometrical (multiple reflections) effect,⁹ and not an actual optical contribution

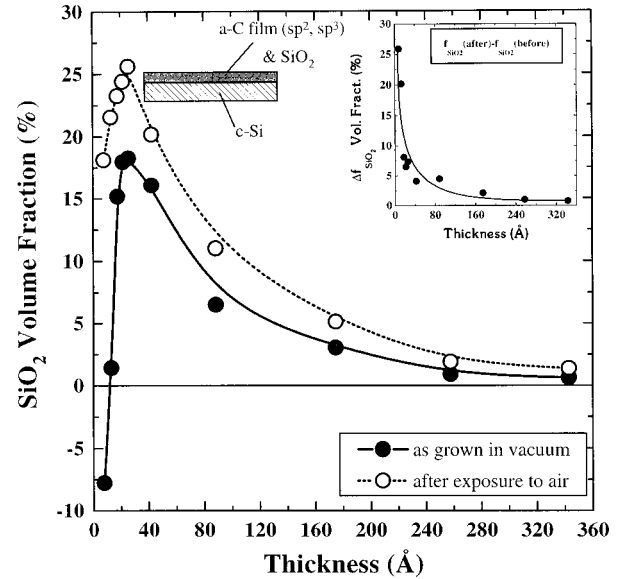


FIG. 2. The calculated SiO₂ contents of *a*-C film vs film thickness, obtained from SE data using the MI model, before (solid circles) and after (open circles) the exposure to air. The inset shows their difference.

from the Si-O or Si-C chemical bonds, since these bonds contribute in the IR region. The abrupt change in $\Delta\langle\epsilon_2\rangle$ from negative to positive values above 3.2 eV occurs because the onset of the interband electronic transitions of the *c*-Si substrate is at this energy region, and the effect of the SiO₂ forms is to reduce the $\langle\epsilon_2\rangle$ values. Especially in the energy region of the E_2 structure, where the penetration depth of the light in *c*-Si is smaller, the measured pseudodielectric function is strongly affected by the existence of this kind of SiO₂ forms either in the bulk *a*-C film or as an overlayer.

In order to get more information about the film oxidation or the formation of a SiO₂ overlayer, the measured $\langle\epsilon\rangle$ spectrum of each deposited layer was analyzed by means of the Bruggeman effective medium theory (EMT), in combination with the three-phase model (air/composite film/*c*-Si substrate) (MI), as well as with the four-phase model (air/SiO₂ overlayer/composite film/*c*-Si substrate) (MII).¹⁰ In MI the deposited layer of thickness d_1 consists of sp^2, sp^3 and SiO₂ components, and in MII of sp^2, sp^3 bonds and voids, whereas the overlayer of thickness d_2 is a mixture of SiO₂ and voids. The reference dielectric functions used in this analysis were taken from Ref. 11 and Ref. 12 for sp^2 and sp^3 components, respectively. We note here that the dielectric function of graphitelike¹¹ material cannot truly describe the sp^2 component and the error deduced from the above analysis is to overestimate its amount. The sp^2 and sp^3 components of the *a*-C film deposited with $V_b = -20$ eV depend on the thickness. The fractions at a film thickness of 345 Å are 51% and 42%, respectively.

Figure 2 presents the calculated SiO₂ contents (f_{SiO_2}) of *a*-C film versus film thickness using the MI model, before and after exposure to air. Their differences (Δf_{SiO_2}) are presented in the inset of the figure and are monotonically reduced. The maximum SiO₂ content appears at ~ 25 Å. Above this thickness there is a progressive reduction, which means that the interdiffusion mechanism is completed, no

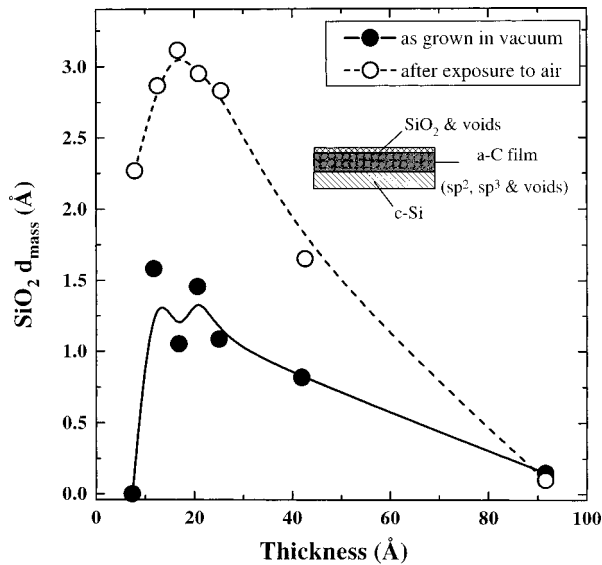


FIG. 3. The calculated SiO_2 mass thickness of the overlayer vs a -C film thickness, obtained from SE data using the MII model, before (solid circles) and after (open circles) the exposure to air.

other SiO_2 is formed and that the calculated SiO_2 content in the film is negligible compared to the volume fractions of sp^2 and sp^3 phases in the film. The physical meaning of the negative SiO_2 volume fraction (-7.5%) obtained for the first deposited layer in vacuum is due to the fact that the deposited layer is more dense than the references we use for sp^2 and sp^3 bonded phases. (Alternatively, it could mean that the references are not the most appropriate to describe the Si-C phases that formed at the initial stages of film growth.)

Using the results obtained from the analysis with the MII model, we calculated the SiO_2 mass thickness ($d_{\text{mass}} = d_2 \times f_{\text{SiO}_2}$) of the overlayer. The evolution of SiO_2 d_{mass} with film thickness is plotted in Fig. 3 for the first seven deposited layers. We can see a drastic reduction of SiO_2 d_{mass} above the first ~ 25 Å of a -C film thickness. The calculated SiO_2 d_{mass} before exposure to air presents an equivalent quantity that yields, when used in the fitting procedure along with the MII model, the mass of SiO_2 trapped within the film during the deposition of the last a -C layer.

We should note here that our attempt to fit the experimental SE data assuming the formation of a SiO_2 interlayer between the c -Si substrate and the a -C film was without success, supporting the argument that Si atoms enter into the film or even reach at the film surface.

The measured internal stresses of the a -C film are shown in Fig. 4 for the sequentially deposited layers to a total thickness of ~ 345 Å. The first deposited layer caused strong deformation of the Si wafer and the subsequently deposited layers lead to stress relaxation. The stress reduction is observed during the first ~ 25 Å. This is the same thickness at which the maximum SiO_2 volume fraction (Fig. 2) in the a -C film and the maximum SiO_2 d_{mass} (Fig. 3) in the overlayer occur. Above this thickness the compressive internal stresses increase as it was expected, because the growing film is rich in sp^3 bonds.¹³ The measured internal stresses for thicknesses below 25 Å are due to the intermixing between the c -Si substrate and the incident C atoms. This reduction is

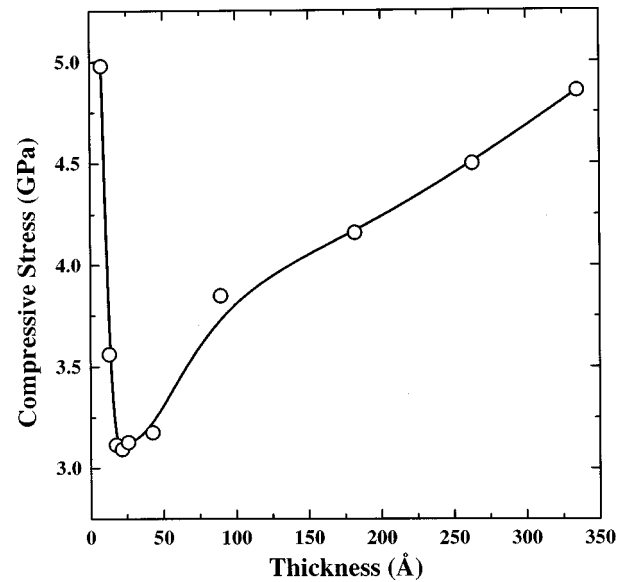


FIG. 4. The evolution of compressive stresses of the a -C film, deposited in sequential layers, with the thickness.

concurrent with the stress relaxation predicted by the theoretical simulations, as will be discussed in the following.

From the above results obtained using the first deposition procedure (growth in sequential layers followed with the exposure to air in order to perform stress measurements), it is evident that the energetic C atoms replace Si atoms in the substrate at the initial stages of growth, forming SiC-like geometries. The replaced Si atoms force their way into the bulk and even the surface of the amorphous layer. After air exposure, the atmospheric O_2 can penetrate through the film surface and form SiO_2 -like geometries, replacing weaker Si-C bonds. It also gives rise to the SiO_2 overlayer, since oxidation mechanisms are more efficient at the surface where mobility is enhanced and Si atoms are even more weakly bonded. This overlayer seems to be resputtered during the deposition of the next layer. For film thickness exceeding ~ 30 Å no formation of an overlayer takes place, because presumably Si atoms cease to diffuse up to the film surface. This is related with the fact that when the film thickness exceeds 25 Å the C atoms do not penetrate into the c -Si substrate, and as a consequence we observe a reduction of the total volume fraction of SiO_2 in the film.

To investigate alterations in the substrate layers, we followed the second procedure outlined in the methodology (growth of sequential layers with no exposure to air). We focus on the differences in the energy region of the E_1 interband transition of c -Si (~ 3.3 eV), which are more pronounced in the second derivative ($d^2\epsilon/d\omega^2$) of the dielectric function.¹⁴ Quantitative analysis provides the energy location (E) and the broadening (Γ) of the E_1 transition.¹⁴ The E and Γ of the ideal case in this heterostructure system (perfect c -Si substrate and a -C film on top, e.g., no compositional disorder at the interface) can be estimated by a fitting process using the Bruggerman EMT in combination with a three-phase (air/composite film/ c -Si substrate) model (MIII), in which the composite a -C film at each thickness consists of sp^2, sp^3 components and voids (but not SiO_2 units). The results of this theoretical analysis, the E and Γ versus thick-

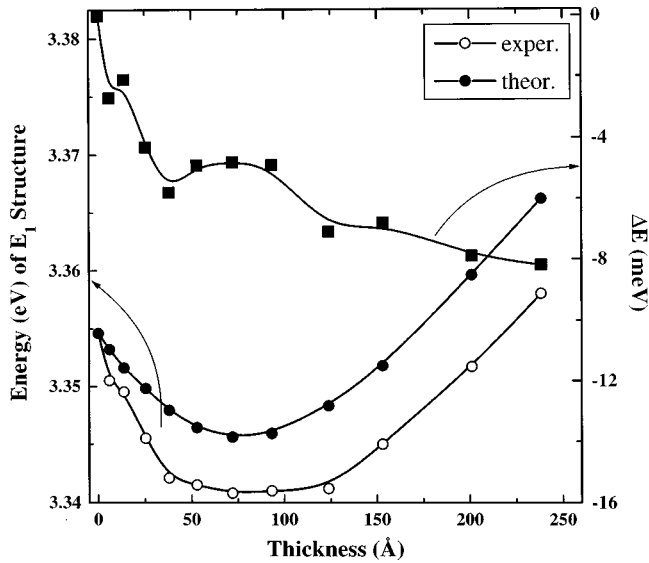


FIG. 5. Energy position (E) of the E_1 transition of c -Si vs thickness of a -C film. Empty (filled) circles show the experimental (model) results (see text), respectively. Filled squares show the differences ΔE .

ness, can then be compared with the actual experimental measurements to detect any deviations from the ideal case.

Figure 5 shows the energy location E versus the thickness of the a -C film. We plot both the experimental (E_{ex}) and the theoretical-model (E_m) results, as well as their difference $\Delta E (=E_{ex} - E_m)$. The latter shows a tendency to decrease with film thickness. This is clear evidence that the growth of the a -C film induces progressively disorder and/or stresses in the substrate and shifts the E_1 position.¹⁵ The reduction of ΔE , especially up to ~ 25 – 30 Å, cannot be considered as a temperature effect because we used the periodic deposition mode, in sequential layers, and we controlled the deposition temperature over a narrow range. For the sake of clarity we mention that the reduction of ΔE due to a temperature effect (energy shift of the E_1 transition to lower energies¹⁶) is only approximately -0.4 meV/°C. Typically, the raise in temperature for long deposition periods above film thickness of 100 Å is of the order of few degrees.

More information about the actual origin of this dependence emerges from the analysis of the broadening of the E_1 structure. Figure 6 shows in a similar fashion the variation of the broadenings Γ with the thickness of the a -C film. The differences $\Delta\Gamma (= \Gamma_{ex} - \Gamma_m)$ signify the presence of disorder in the substrate. We observe an increase of the experimental Γ for the first ~ 25 – 30 Å, and after that a reduction compared to that of bulk c -Si. The initial effect (broadening increase) is related to incident energetic C atoms that penetrate into the substrate and replace Si atoms at substitutional positions. This nicely explains the simultaneous diffusion of Si atoms out and into the amorphous film. The growth of thicker films leads to the broadening reduction, which can only be associated with the development of high uniaxial stresses along the (111) direction of the c -Si substrate.¹⁷ We should note here that even though the uncertainties in the calculated Γ are ≤ 1 meV, and thus the $\Delta\Gamma$ uncertainties are of the order of the absolute values, the trend of the dependence of $\Delta\Gamma$ on film thickness is obvious. Figure 7 dis-

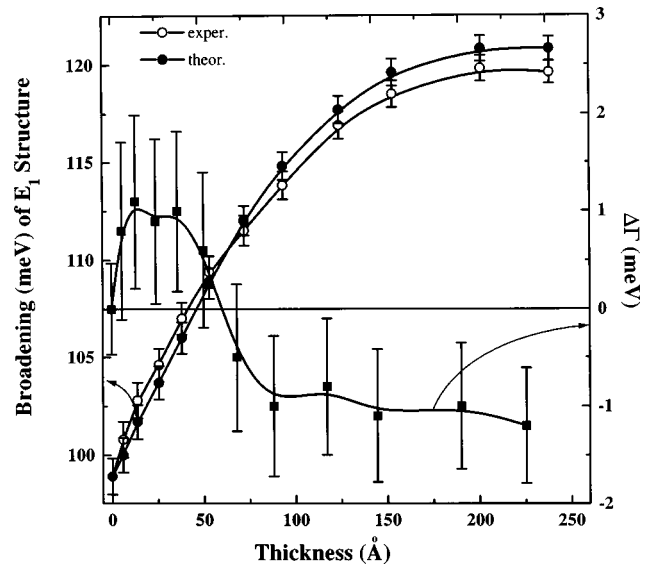


FIG. 6. Broadening (Γ) of the E_1 transition of c -Si vs thickness of a -C film. Empty (filled) circles show the experimental (model) results (see text), respectively. Filled squares show the differences $\Delta\Gamma$.

plays the interrelation between the compressive stress of the a -C film and the $\Delta\Gamma$ of the c -Si substrate. The data clearly indicate that the reduction in $\Delta\Gamma$ is caused by the increased intrinsic compressive stress of the rich in sp^3 sites a -C film.

B. Theoretical simulations

Our experimental observations and the accompanying analysis presented above suggest that interdiffusion of species across the interface during the initial stages of growth is taking place. To gain a deeper insight into the experimental observations and verify this phenomenon, we performed theoretical simulations of the interface equilibrium structure using the MC procedure outlined in detail in the methodology section.

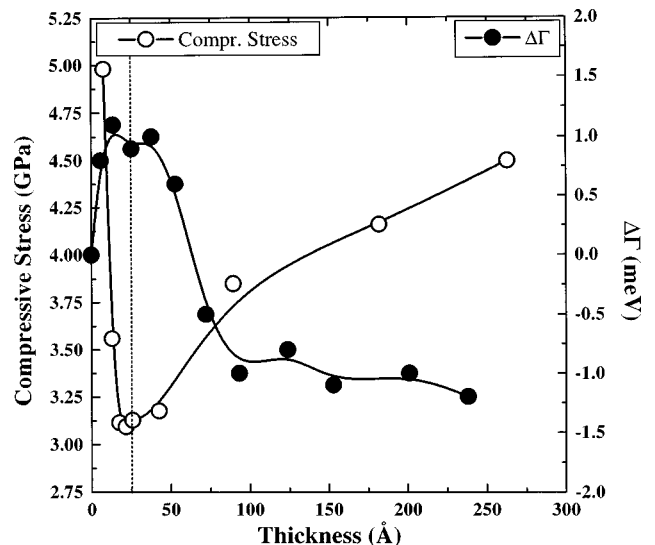


FIG. 7. Comparison of internal compressive stresses (left axis, open circles) presented in Fig. 4, with the differences $\Delta\Gamma$ (right axis, filled circles) shown in Fig. 6.

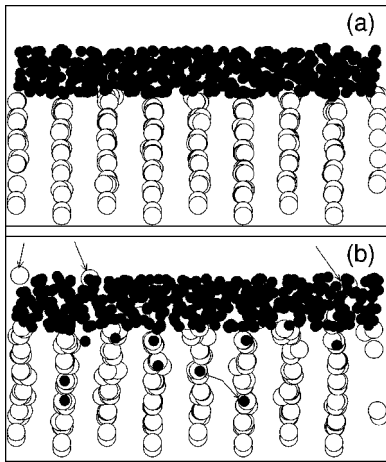


FIG. 8. Illustration of a 12-Å a -C film on top of the c -Si(100) substrate, (a) before and (b) after interdiffusion. Atomic positions are projected on the (010) plane of the tetragonal cell. Filled small circles are carbon atoms. Open large circles are silicon atoms. Few interdiffused atoms are indicated by arrows.

We first examine the possibility for interdiffusion by considering composite structures at an early stage of growth. Typical thicknesses of the a -C film studied range from 2 Å (the first one or two ‘‘monolayers’’ of carbon on the c -Si substrate) up to ~ 15 Å. The structure with the thickest a -C film (14.5 Å) contains 672 atoms, of which 288 are Si atoms in the c -Si substrate (24 layers of 12 atoms each; this number remains fixed for all structures), and 384 are C atoms in the a -C film. Expectedly we find that the average coordination \bar{z} of the a -C film rises as the thickness becomes larger. So, for the thinnest film ($d_{thick} \approx 1.8$ Å) we find $\bar{z} \approx 3.1$, while for $d_{thick} \approx 14.5$ Å the film has already acquired diamondlike nature with $\bar{z} \approx 3.5$. This trend can be understood by realizing that the thinner the film, the more easy to relax the compressive stresses near the interface that are responsible for promoting tetrahedral bonding (see discussion below).

Pictorial evidence for compositional disorder at the interface is given in Fig. 8 which portrays a typical composite structure at an initial stage of growth, both before and after the particle exchange process. Atomic positions indicate average site occupancies. (a) shows the ideal interface that is highly strained (to be discussed below). (b) shows the resulting configurations after allowing interdiffusion. We most clearly see C atoms diffusing into substitutional sites in the substrate and forming SiC-like geometries. No C-C bonds are formed. Recently, Kelires and Kaxiras demonstrated⁷ that the strain field induced by the *surface reconstruction* and the C-C interactions in $\text{Si}_{1-x}\text{C}_x(100)$ thin layers drive the diffusion-in of adsorbed C atoms. Here, we show that the presence of the *strained interface* drives a similar, but simpler effect. In the case of the reconstructed surface, the strain field in the near surface region is strongly inhomogeneous with marked site dependence.¹⁸ In the present case, there is no such dependence and as a result the C atoms do not show preference for specific sites in the substrate layers. Still, C atoms avoid each other as nearest neighbors, while they have a preferred third-nearest neighbor arrangement in the Si lattice, as found before.^{4,19}

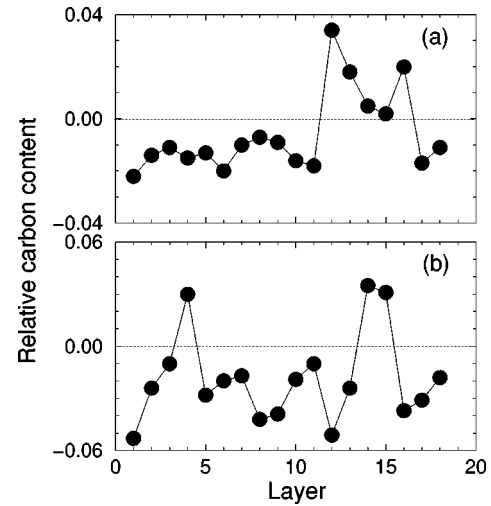


FIG. 9. Equilibrium depth profile of carbon atoms (at 800 K) in the substrate of two composite structures. The a -C layer is ~ 2 Å thick in (a) and ~ 4 Å thick in (b). 1/2 and 1 ML of C atoms are diffused, respectively. Carbon content is given relative to a hypothetical average layer composition.

Si atoms are also shown to diffuse into the amorphous thin layer. This is expected since diffusion in our approach is the result of mutual particle exchanges. Of course we are sampling the equilibrium configurations, atoms are found in the favorable end-of-diffusion state, we do not follow the actual trajectories and intermediate states. The physical picture is the following: an energetic carbon atom at the initial stage of growth (being close to the interface) enters into the Si substrate, it diffuses a certain distance and kicks out a Si atom from a substitutional position. (The possibility of interstitial C is not examined; the ratio interstitial/substitutional carbon in Si becomes significant only at high C contents). The Si atom instead of staying interstitial in the substrate, which costs energy, prefers to diffuse into the amorphous carbon film to form Si-C bonds. We can see from Fig. 8 that Si atoms can even reach the less energetically favorable surface environment. Thus, we arrive at a picture where the possibility of bulk oxidation and the formation of SiO_2 surface units, as suggested by our experimental observations, are accounted for by the MC simulations.

To obtain a more quantitative picture of the intermixing process, we calculated the equilibrium depth profile of C atoms in the substrate layers. This is shown in Fig. 9 for two distinct cases, typical for the very early stages of growth. To study the effect of the amount of C in the substrate, we allow diffusion of the equivalent of 1/2 ML of C in the structure of (a), and 1 ML of C in the structure of (b). We first compute an average site occupancy in the 18 substrate layers, where diffusion is permitted, and then we average in every layer. The C content is given relative to the value that corresponds to spreading 1/2 or 1 ML of C over 18 layers. The most interesting feature of the profile in both cases is an oscillatory behavior which separates C-enriched layers from C-depleted ones. The first layer at the interface is strongly depleted from C. Enrichment occurs away from the interface, even in the case of (b) with more C atoms in the substrate, indicating a repulsion among diffused C and the amorphous film. A similar but more complex, due to the surface

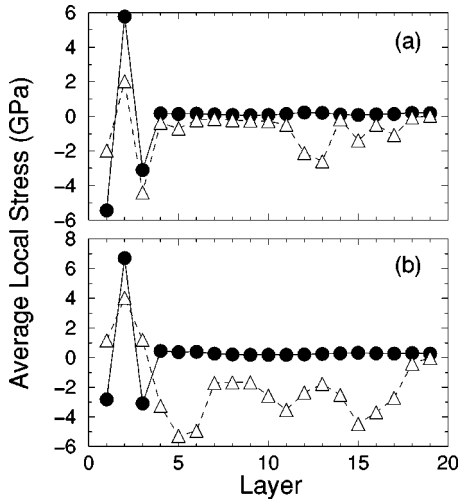


FIG. 10. Average local atomic stresses in the structures of Fig. 9. The layer numbered 1 denotes the whole amorphous film, the rest are monolayers in the *c*-Si substrate. Filled (empty) symbols show stresses before (after) intermixing, respectively.

reconstruction, oscillatory behavior has also been observed in the *c*-Si_{1-x}C_x(100) system.⁷ We attribute this behavior to the repulsive interaction between nearest-neighbor C atoms in the Si lattice,⁴ which prevents them from equally populating adjacent layers.

To get a deeper insight into the driving force behind this effect, we examine the strain and the energetics of the interfacial system. Strain plays a very important role in such mismatched systems. For this purpose, we utilize the concept of local atomic stresses that has been very useful in exploring the elastic properties of *a*-C networks.⁸ Atomic level stresses are a measure of the local rigidity of the network. They can be thought of as arising due to local incompatibilities, and they are present in networks with nonequivalent atoms and in any disordered structure. They are derived by considering an atomic compression (or tension) at each site given by $\sigma_i = -dE_i/d\ln V \sim p\Omega_i$, where E_i is the energy of atom i (as obtained by decomposition of the total energy into atomic contributions), and V is the volume. Dividing by the appropriate atomic volume Ω_i converts into units of pressure p_i . For each atom we compute the average atomic stress $\bar{\sigma}_i$, both before and after interdiffusion. Then atomic contributions are summed up to give the average stress in the whole *a*-C layer, as well as in every individual substrate layer.

Figure 10 plots the depth profile of average stress for the two cases whose C profile is sketched in Fig. 9. Negative values are for tensile, while positive values are for compressive stress. We find, for the ideal interface and in both cases, tensile average stress in the amorphous film because carbon atoms at the interface are stretched to make bonds with the topmost Si atoms of the substrate. The thinner the film the larger the tensile stress, as the interface contribution overwhelms stresses from the rest of the amorphous layer. (The effect fades as the thickness increases, see below). On the other hand, the first substrate layer at the interface is under compression to compensate for the stress conditions above. The Si atomic volumes in this layer are shrunk compared to the ideal value to accommodate for bonding with the smaller

carbon atoms. The same effect enforces the second layer in the substrate to be under tension. Deeper layers have nearly zero average stress.

The situation changes drastically after intermixing. It is obvious that diffusion is a strain mediated mechanism. Stresses are considerably relieved both in the thin amorphous layer as well as in the substrate layers near the interface, which evidently tends to relax its strain. At the same time tensile stresses are generated at deeper layers in the substrate, exactly where C substitutionals are introduced (compare Figs. 9 and 10). The *interdiffused state*, however, is energetically favored despite the induction of stresses in the substrate, because these stresses are overwhelmed by the reduction near the interface. We compute an average energy gain of $\sim 40 \pm 10$ meV/atom, compared to the ideal state.

When the *a*-C film thickness increases, the average stress in the film progressively acquires compressive values (after $\sim 7-8$ Å), as the effect of the interface generating tensile stresses nearby cannot overwhelm the compressive stresses generated above. The important point is that in this case as well, as in the case of initially tensile amorphous layer, the stress is partly relieved after the interdiffusion process. For example, the *a*-C layer with thickness $d_{thick} \approx 14.5$ Å and $\bar{z} \approx 3.5$ has after formation under pressure, without annealing at higher temperature, and before intermixing a $\bar{\sigma}_{a-C} \approx 9$ GPa. After intermixing, the compressive stress is reduced to $\bar{\sigma}_{a-C} \approx 5$ GPa. So, intermixing and stress relaxation are closely associated in the early stages of growth, in agreement with our experimental observations.

Finally, let us point out that interdiffusion may bear significance for the growth of thicker amorphous layers with high sp^3 content. It has been shown previously that a correlation exists at the local atomic level between stress conditions and C hybridization.⁸ Tensile conditions favor the formation of sp^2 sites, while sp^3 sites are most likely being formed under compressive conditions. The important point here is the reduction of tensile stress in the interface region, at the very early stages of growth, following intermixing. This enhances the chance that further deposited material will acquire diamondlike nature. If, however, the experimental conditions do not favor or inhibit intermixing, this would leave the interface in a stressed state and lead to the creation of a thick graphitic layer near the interface. The control of the thickness of this interface layer might be crucial for the successful fabrication of thin film transistor devices based on ta-C.²⁰

IV. CONCLUSIONS

We showed in this paper that our complementary experimental spectroscopic ellipsometry and stress measurements and theoretical MC simulations are powerful tools for the investigation of the interfacial properties of thin amorphous films. We apply the methodology to *a*-C films grown on Si(100) substrates, where we monitor the interdiffusion by probing the compositional and stress profiles across the interface and by identifying the relevant atomistic processes.

ACKNOWLEDGMENTS

This work was supported in part by the EU EPET II 333 project.

- ¹P.C. Kelires, Phys. Rev. B **49**, 11 496 (1994); D.E. Jesson, S.J. Pennycook, and J.M. Baribeau, Phys. Rev. Lett. **66**, 750 (1991).
- ²S. Logothetidis, Appl. Phys. Lett. **69**, 158 (1996).
- ³R. Azzam and N. Bashara, *Ellipsometry and Polarized Light* (North Holland, Amsterdam, 1977).
- ⁴P.C. Kelires, Phys. Rev. Lett. **75**, 1114 (1995).
- ⁵P.C. Kelires, Int. J. Mod. Phys. C **9**, 357 (1998).
- ⁶J. Tersoff, Phys. Rev. B **39**, 5566 (1989).
- ⁷P.C. Kelires and E. Kaxiras, Phys. Rev. Lett. **78**, 3479 (1997).
- ⁸P.C. Kelires, Phys. Rev. Lett. **73**, 2460 (1994).
- ⁹D.E. Aspnes, in *Optical Properties of Solids—New Developments*, edited by B.O. Seraphin (North-Holland, Amsterdam, 1976), p. 799.
- ¹⁰D.E. Aspnes, Thin Solid Films **89**, 249 (1982).
- ¹¹S. Logothetidis, J. Petalas, and S. Ves, J. Appl. Phys. **79**, 1040 (1996).
- ¹²F. Xiong, Y.Y. Wang, and R.P.H. Chang, Phys. Rev. B **48**, 8016 (1993).
- ¹³S. Logothetidis and M. Gioti, Mater. Sci. Eng. B **46**, 119 (1997).
- ¹⁴L. Vina, S. Logothetidis, and M. Cardona, Phys. Rev. B **30**, 1979 (1984).
- ¹⁵S. Logothetidis, H.M. Polatoglou, and S. Ves, Solid State Commun. **68**, 1075 (1988).
- ¹⁶P. Lautenschlager, M. Garriga, L. Vina, and M. Cardona, Phys. Rev. B **36**, 4821 (1987).
- ¹⁷P. Etchegoin, J. Kircher, and M. Cardona, Phys. Rev. B **47**, 10 292 (1993).
- ¹⁸P.C. Kelires and J. Tersoff, Phys. Rev. Lett. **63**, 1164 (1989).
- ¹⁹H. Rücker, M. Methfessel, E. Bugiel, and H.J. Osten, Phys. Rev. Lett. **72**, 3578 (1994).
- ²⁰C.A. Davis, K.M. Knowles, and G.A.J. Amaratunga, Surf. Coat. Technol. **76-77**, 316 (1995).